

## ORIGINAL ARTICLE

# LiCl attenuates impaired learning and memory of APP/PS1 mice, which in mechanism involves $\alpha 7$ nAChRs and Wnt/ $\beta$ -catenin pathway

Jie Xiang<sup>1,2</sup> | Long-Yan Ran<sup>1,2</sup> | Xiao-Xiao Zeng<sup>1,2</sup> | Wen-Wen He<sup>1</sup> | Yi Xu<sup>2</sup> | Kun Cao<sup>2</sup> | Yang-Ting Dong<sup>2,3</sup> | Xiao-Lan Qi<sup>2,3</sup> | Wen-Feng Yu<sup>2,3</sup> | Yan Xiao<sup>2,3</sup> | Zhi-Zhong Guan<sup>1,2,3</sup> 

<sup>1</sup>Department of Pathology, Guizhou Medical University and the Affiliated Hospital of Guizhou Medical University, Guiyang, P.R. China

<sup>2</sup>Key Laboratory of Endemic and Ethnic Diseases, Ministry of Education, Guizhou Medical University, Guiyang, P.R. China

<sup>3</sup>Provincial Key Laboratory of Medical Molecular Biology, Guiyang, P.R. China

## Correspondence

Zhi-Zhong Guan, Department of Pathology at the Affiliated Hospital, and the Key Laboratory of Endemic and Ethnic Diseases of the Ministry of Education, Guizhou Medical University, Guiyang, 550004, P. R. of China.  
Email: 1457658298@qq.com

## Funding information

This work was supported by the Natural Science Foundation of China (grant number U1812403); the Foundation of Guizhou Province of China (grant numbers 2014-06, 2014-6008, 2016-4001, 2018-5779-5 and YJSCXJH 2020-149)

## Abstract

We examined the mechanism by which lithium chloride (LiCl) attenuates the impaired learning capability and memory function of dual-transgenic APP/PS1 mice. Six- or 12-month-old APP/PS1 and wild-type (WT) mice were randomized into four groups, namely WT, WT+Li (100 mg LiCl/kg body weight, gavage once daily), APP/PS1 and APP/PS1+Li. Primary rat hippocampal neurons were exposed to  $\beta$ -amyloid peptide oligomers (A $\beta$ Os), LiCl and/or XAV939 (inhibitor of Wnt/ $\beta$ -catenin) or transfected with small interfering RNA against the  $\beta$ -catenin gene. In the cerebral zone of APP/PS1 mice, the level of A $\beta$  was increased and those of  $\alpha 7$  nicotinic acetylcholine receptors (nAChR), phosphor-GSK3 $\beta$  (ser9),  $\beta$ -catenin and cyclin D1 (protein and/or mRNA levels) reduced. Two-month treatment with LiCl at ages of 4 or 10 months weakened all of these effects. Similar expression variations were observed for these proteins in primary neurons exposed to A $\beta$ Os, and these effects were attenuated by LiCl and aggravated by XAV939. Inhibition of  $\beta$ -catenin expression lowered the level of  $\alpha 7$  nAChR protein in these cells. LiCl attenuates the impaired learning capability and memory function of APP/PS1 mice via a mechanism that might involve elevation of the level of  $\alpha 7$  nAChR as a result of altered Wnt/ $\beta$ -catenin signalling.

## KEYWORDS

APP/PS1 mice, A $\beta$ Os, LiCl, Wnt/ $\beta$ -catenin signalling pathway,  $\alpha 7$  nAChR

## 1 | INTRODUCTION

As the most frequently occurring ageing-related dementia, Alzheimer's disease (AD) features progressive loss of cognitive abilities, in particular learning and memory.<sup>1</sup> The hallmarks of this disease in the brain include intracellular tau (highly

phosphorylated)-containing neurofibrillary tangles, extracellular  $\beta$ -amyloid peptide (A $\beta$ )-containing amyloid plaques, an excessive loss of synapses and deficient cholinergic transmission.<sup>2</sup>

The 'cholinergic hypothesis' proposes that among AD patients observed, decreased cholinergic innervation is a contributing factor of cognitive degradation.<sup>3</sup> The nicotinic acetylcholine receptors (nAChRs)

This is an open access article under the terms of the Creative Commons Attribution License, which permits use, distribution and reproduction in any medium, provided the original work is properly cited.

© 2021 The Authors. *Journal of Cellular and Molecular Medicine* published by Foundation for Cellular and Molecular Medicine and John Wiley & Sons Ltd.

of neurons participate in cognitive processing, as well as learning and memory. Expression alterations in these receptors are associated with the impaired cholinergic neurotransmission<sup>4</sup> and may be responsible for complex neuronal diseases such as AD and Parkinson disease.<sup>5</sup>

Indeed, nAChRs level is lowered in the cerebral zone of the AD patients and of animal models of this disease, as well as in isolated neuronal cells exposed to A $\beta$ .<sup>6,7</sup>  $\alpha$ 7, the main subtype of nAChR present in both neuronal and non-neuronal cells of the human brain consists mainly of five  $\alpha$ 7 subunits and is considered to be one of the receptors most closely associated with the AD contraction.<sup>8</sup> A $\beta$ <sub>1-40</sub> and A $\beta$ <sub>1-42</sub> bind to  $\alpha$ 7 nAChR with an affinity in the nanomolar range, resulting in gradual depletion and inactivation of this receptor.<sup>9</sup>

In addition to the toxic consequences due to the direct nAChRs binding by A $\beta$ , other subcellular events have been associated with AD, including down-regulation of canonical axis Wnt/ $\beta$ -catenin, which might influence the stability of these receptors. When Wnt receptors are not activated, the  $\beta$ -catenin bound by Axin is phosphorylated in succession via glycogen synthase kinase-3 $\beta$  (GSK3 $\beta$ ) and casein kinase 1 at a range of Ser/Thr residues (regularly spaced), which are located at the N-terminus of the  $\beta$ -catenin. Consequently, ubiquitination and targeting of  $\beta$ -catenin are initiated for fast disruption by proteasome, thereby depressing the expression of downstream targets such as cyclin D1.<sup>10</sup>

Interestingly, Wnt/ $\beta$ -catenin signalling is closely linked to learning capability and memory function among mammals and this signalling is impaired both in the brains of AD patients,<sup>11</sup> as well as animal AD models.<sup>12</sup> This dysfunction exerts a crucial effect on the neuronal degeneration, as well as the impairment of synapses, creating a deleterious pathway that leads to dementia.<sup>13</sup> Notably, nAChRs are present both on presynaptic<sup>14</sup> and on postsynaptic<sup>15</sup> membranes, and loss of these receptors leads inevitably to abnormalities in synapses. Furthermore, when the Wnt signalling pathway is activated persistently via ligand medication or suppressor deactivation, it overcomes the toxic effects of A $\beta$  and improves cognitive performance in patients with AD.<sup>16,17</sup>

As is widely acknowledged, lithium is the preferred mood-stabilizing agent for maintaining bipolar disorder.<sup>18</sup> Apart from stabilizing moods, lithium can also resist suicidal thoughts, regulate immunity and protect nerve system,<sup>19</sup> which, during the last decade, has come to be regarded as a neuroprotective agent and is now widely used in studies of neurodegenerative diseases, including AD.<sup>20</sup> It is noteworthy in this context that the incidence of AD among patients with bipolar disorder who have been taking lithium is lower than among those not undergoing lithium therapy.<sup>18</sup> Lithium chloride (LiCl) inhibits GSK3 $\beta$ , thereby reducing this activity in the brain of animal models of AD, while enhancing Wnt/ $\beta$ -catenin signalling.<sup>21,22</sup>

Accordingly, lithium may be of value in treating AD. However, it is currently unknown whether lithium can reverse the learning and memory impairments in murine AD model and, if so, whether this effect involves Wnt/ $\beta$ -catenin signalling modulation, as well as consequent regulation of  $\alpha$ 7 nAChR. Here, we investigated these questions by treating both APP/PS1 transgenic mice and  $\beta$ -amyloid peptide oligomer (A $\beta$ O)-exposed primary neurons using LiCl or XAV939, a small

molecule selective inhibitor that promotes  $\beta$ -catenin degradation and inhibits the transcription by  $\beta$ -catenin,<sup>23</sup> and then analysing the cognitive ability of these mice, as well as potential changes in Wnt/ $\beta$ -catenin and  $\alpha$ 7 nAChR in both of these systems.

## 2 | MATERIALS AND METHODS

### 2.1 | Materials

LiCl, A $\beta$ <sub>1-42</sub> and XAV939 (Sigma-Aldrich Inc.); anti-A $\beta$  mouse monoclonal antibody (BioLegend Inc.); anti-GSK3 $\beta$ , anti-phosphor-GSK3 $\beta$  (ser9), anti-cyclin D1 and anti- $\beta$ -catenin rabbit monoclonal antibodies, as well as horseradish peroxidase (HRP)-conjugated anti-rabbit IgG (Cell Signaling Technology); anti-GAPDH rabbit polyclonal antibody (Genetex); anti-nAChR  $\alpha$ 7 rabbit polyclonal antibody (Abcam); cell counting Kit-8 (Dojindo Molecular Technologies); anti-NeuN mouse monoclonal antibody (Merck Millipore); anti-gial fibrillary acidic 113 protein (GFAP) rabbit monoclonal antibody (Dako); CY-3-labelled anti-mouse IgG and 488-labelled anti-rabbit IgG (Thermo scientific Inc.); A $\beta$ <sub>42</sub> assaying kits (Thermo scientific Inc.); Lipofectamine RNAiMAX Reagent (Invitrogen Inc.); universal 2 $\times$ PCR mastermix (TaqMan; Applied Biosystems); and the remaining chemicals were all procured from Sigma-Aldrich.

### 2.2 | Experimental animals

B6.Cg-Tg (PSEN1dE9 and APP<sub>SWE</sub>) mice aged 4 months having a 85Dbo/Mmjax background were procured from Nanfang BioTechnology Co., Ltd. Meanwhile, wild-type (WT) mice of identical strain were also procured from the same company. All mice were 20–30 g in body weight. Each male mouse was allowed to mate with four females. When the resulting pups were 12–20 days old, the tips of their tails were cut off for extraction of DNA and the polymerase chain reaction (PCR)-based genotyping, where agarose gel electrophoresis (1.5%) was used for product analysis. For PCR primer design of target transcripts shown in Table 1, the entire cDNA sequences from GenBank were consulted.

The described experimental procedures in this study have all been approved by the Ethical Committee of Guizhou Medical University in China (no. 1702110).

Based on literature and the results of previous studies,<sup>24,25</sup> the 4- or 10-month-old WT and transgenic (APP/PS1) mice were randomized into

TABLE 1 The primers used for amplification of mouse APP and PS1 cDNA

Gene	Sequence of primers	Length (bp)
APP	For 5'-GACTGACCACTCGACCAGGTTCTG-3'	400
	Rev 5'-CTTGAAGTTGGATTCTCATATCCG-3'	
PS1	For 5'-AATAGAGAACGGCAGGAGCA-3'	608
	Rev 5'-GCCATGAGGGCACTAATCAT-3'	

four groups (six animals in each) for subsequent treatment for 2 months as follows: (1) the WT group: WT animals received gavage normal saline at about 0.4 ml once per day; (2) the WT+Li group: 100 mg/kg LiCl was administered to the WT animals; (3) the APP/PS1 group: normal saline was given to the animals with APP/PS1 double mutations in identical manner to group (1); (4) the APP/PS1+Li group: transgenic animals were treated with LiCl in the same manner as group (2).

### 2.3 | Culturing and treatment of primary hippocampal neurons

Primary neurons were obtained from the cerebral zone of newborn Sprague-Dawley rats employing minor modifications of a published procedure.<sup>26</sup> For purity assessment of these primary neurons, immunofluorescent double staining was performed in succession using the anti-NeuN mouse antibody, the CY-3-labelled anti-mouse IgG (red), the anti-GFAP rabbit antibody and a subsequent 488-labelled anti-rabbit IgG (green).

A $\beta$ O<sub>42</sub> were prepared by a procedure described earlier<sup>27</sup> and the suitable concentration for exposure chosen as also described previously.<sup>26</sup> Initially, cell exposure to varying doses of LiCl (0–100 mmol/L) and XAV939 (0–50  $\mu$ mol/L) was accomplished for different times. Thereafter, the cells were subjected to 2-h incubation with CCK8 solution (10  $\mu$ l), following which the absorption at 450 nm was determined.

Transfection with small interfering RNA (siRNA) was initiated by adding a mixture (1:1) of Lipofectamine RNAiMAX Reagent diluted in Opti-MEM Medium (15  $\mu$ l:250  $\mu$ l) and the siRNA (For 5'-GACUACCUGUUGUGGUUAAAdTdT-3'; Rev 5'-UUAACCACAAAGGUAGUCdTdT-3'), also diluted in Opti-MEM Medium (1:50) for 5 min. Then, the cells were incubated with the siRNA-Lipid complex for 48 h at 37°C.<sup>28</sup>

### 2.4 | Morris water maze for spatial learning and memory

In a 25–26°C water-filled round pool rendered opaque using milk powder, every mouse was compelled to find an underwater escape facility.<sup>29</sup> In the familiarization and acquisition sessions, 60 s was offered for every mouse to seek the hidden facility, and then, 5 s was offered to keep seated on the facility. Afterwards, the mice returned to the original cage. In the retention session, where the facility was withdrawn from the pool, the path adopted by every mouse was video recorded for 60 s, in order to determine the time expenditure for swimming to the original facility location, and the number of passes across and the time expenditure at this location.

### 2.5 | Determination of A $\beta$ <sub>42</sub> by ELISA

The murine cerebral level of A $\beta$ <sub>42</sub> was determined utilizing a murine A $\beta$ <sub>42</sub> ELISA kit as per the protocol of manufacturer.<sup>29</sup> Briefly, after homogenization and centrifugation of the tissue, the pellets obtained

were extracted with 5 M guanidine-HCl. After dilution of aliquot protein from each extract to an ultimate volume (100  $\mu$ l), 2-h incubation was accomplished in plate wells under the room temperature (RT) condition. Next, the wells were rinsed, injected with solution of Detection Antibody (100  $\mu$ l) and then incubated for one more hour at RT. Thereafter, the wells were again washed, followed by 30-min incubation using solution of HRP-linked antibody (100  $\mu$ l) and four extra washes. The last step involved addition of stop solution and absorbance measurement (450 nm) with a spectrophotometer (Bio-Rad Inc.).

### 2.6 | Quantification of the levels of phospho-GSK3 $\beta$ (ser9), GSK3 $\beta$ , $\beta$ -catenin, cyclin D1 and $\alpha$ 7 nAChR by Western blotting

Brain tissue or cultured cells in lysis buffer containing a mixture of protease inhibitors were disrupted in a glass homogenizer. The resulting homogenate was subjected to 20-min centrifugation under 4°C and 15520 g conditions. For the resulting supernatants, the BCA protein assaying kit was utilized to measure the protein concentrations.<sup>26</sup> Afterwards, protein isolation was performed via 10% SDS-PAGE. Finally, a transfer unit (Bio-Rad Inc.) was utilized to blot the protein isolates onto the polyvinylidene difluoride (PVDF) films.

To achieve relative protein quantization, the above PVDF membranes were then subjected to incubation using antibodies against phospho-GSK3 $\beta$  (ser9), GSK3 $\beta$ ,  $\beta$ -catenin, cyclin D1,  $\alpha$ 7 nAChR or GAPDH overnight at 4°C. Next, the membranes were rinsed and subjected to 60-min incubation using secondary antibody conjugated to HRP. Subsequently, enhanced chemiluminescence kit (Millipore) was used to detect the protein bands, and visualization of the resulting signals was accomplished for 30 s–3 min by exposing to chemiluminescence film (hyperperformance). Signal intensity was quantified employing the Image J software.

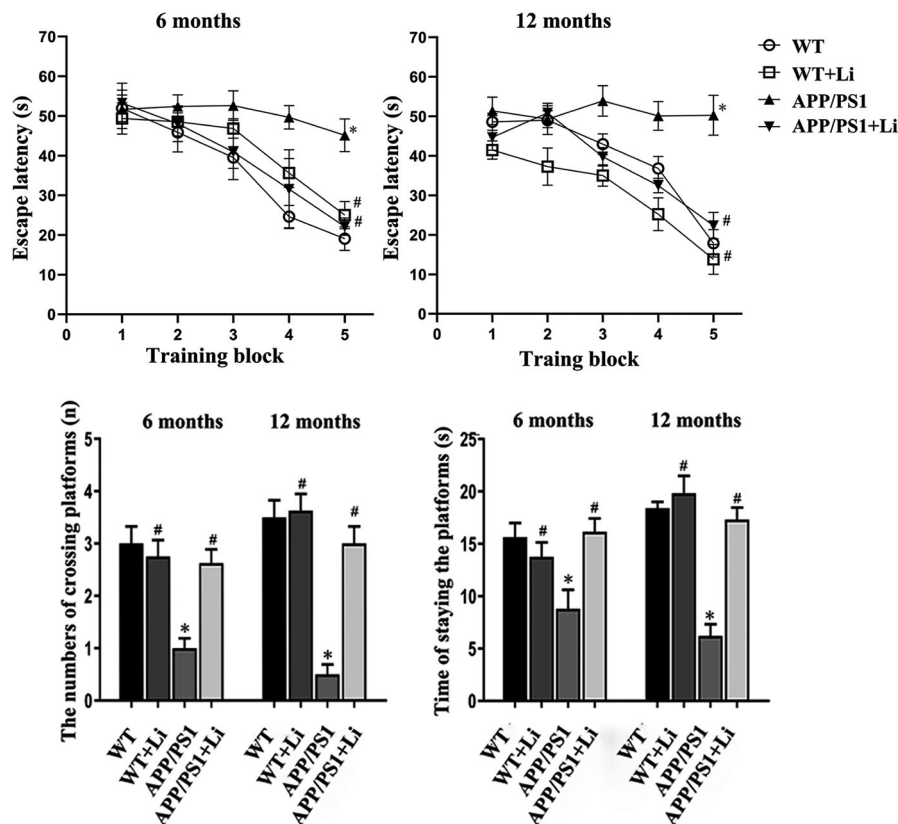
### 2.7 | Determination of the level of $\alpha$ 7 nAChR mRNA by reverse transcription and quantitative real-time PCR

Total RNA, which was extracted via Trizol Reagent from brain tissue or cells, was used to obtain cDNA by reverse transcription with the Prime Script™ RT Master Mix cDNA Synthesis Kit (Takara Bio).<sup>30</sup> A Sequence Detection System (ABI PRISM 7300; Applied Biosystems) was utilized to perform quantitative real-time PCR as per the protocol of manufacturer. Then, the PCR analysis was accomplished with the aid of GeneAmp7300 SDS. The level of  $\alpha$ 7 nAChR transcripts was estimated using  $2^{-\Delta\Delta CT}$  (RQ value) and the formula  $\Delta\Delta CT = \Delta CT_{\text{target}} - \Delta CT_{\text{control}} = (CT_{\text{target}} - CT_{\text{GAPDH}}) - (CT_{\text{control}} - CT_{\text{GAPDH}})$  with the error estimate being  $\Delta\Delta CT$  plus and minus the standard deviation. The sequences of the PCR primers utilized are presented in Table 2. The level of GAPDH mRNA was used as the internal control.

**TABLE 2** The primers used for amplification of mouse or rat  $\alpha 7$  nAChR cDNA

Species	Gene	Sequence of primers	Length (bp)
Rat	$\alpha 7$ nAChR	For 5'-CGGAGTGAAGAATGTTCTGTTTT-3' Rev 5'-GAATATGCCTGGAGGGAGATAC-3'	241
Mouse	$\alpha 7$ nAChR	For 5'-CACATTCCACACCAACGTCTT-3' Rev 5'-AAAAGGGAACCAGCGTACATC-3'	106
Rat	GAPDH	For 5'-GACATGCCGCTGGAGAAAC-3' Rev 5'-AGCCCAGGATGCCCTTTAGT-3'	92
Mouse	GAPDH	For 5'-GGTTGTCTCTCGACTTCA-3' Rev 5'-TGGTCCAGGTTTCTTACTCC-3'	183

**FIGURE 1** Morris water maze assessments of the learning capability and memory function among 6- or 12-month-old WT and dual-transgenic APP/PS1 mice. The four groups were subjected to 2-month gavage administration once daily as follows: WT: WT mice received physiological saline (PS); WT+Li: WT mice received LiCl (Li); APP/PS1: transgenic mice received PS; APP/PS1+Li: transgenic mice received Li. The values are represented as means  $\pm$  SDs ( $n = 6$ ), \* $p < 0.05$  as compared to WT; # $p < 0.05$  as compared to APP/PS1 mice



## 2.8 | Examination of senile plaques and $\alpha 7$ nAChR by immunohistochemical or immunofluorescent staining

Immunohistochemical staining for senile plaques and  $\alpha 7$  nAChR in the brains of mice was accomplished by consulting prior literature.<sup>31</sup> Initially, sections were deparaffinized and dehydrated. Next, they were subjected to 20-min microwaving with pH 6.0 citric acid buffer (0.01 M) for antigen retrieval, followed by 30-min placement in blocking medium (Dako Inc.) under RT condition. Afterwards, overnight incubation of sections was accomplished at 4°C using anti-A $\beta$  and anti- $\alpha 7$  nAChR antibodies. The next day, incubation was further carried out using rabbit IgG or goat anti-mouse biotinylated antibody under RT condition for 60 min. Afterwards, further incubation was accomplished using the avidin/biotinylated enzyme complex, followed

by placement in diaminobenzidine-containing peroxidase reaction buffer. Aided by Image Pro Plus, we quantified the number of senile plaques and integral optical density (IOD) of  $\alpha 7$  nAChR staining in stochastically selected visual fields under a  $\times 200$  original magnification.

For immunostaining of  $\alpha 7$  nAChR in isolated cells, seeding of primary neurons was done onto six-well plates coated with polylysine, followed by three times of washing in PBS and paraformaldehyde fixation (4%). Then, these samples were subjected to 30-min treatment with goat serum at RT and a subsequent overnight incubation with antibody against  $\alpha 7$  nAChR at 4°C.<sup>26</sup> The next day, incubation was further carried out with fluorescein isothiocyanate-labelled anti-rabbit goat IgG (488-labelled) for 1 h at RT. Afterwards, the cells were subjected to three times of PBS rinsing and coversliping with Vectashield (Vector Laboratories). Aided by Image Pro Plus, we quantified the IOD of immunofluorescent staining for  $\alpha 7$

nAChR in stochastically selected visual fields under a  $\times 400$  original magnification.

## 2.9 | Statistical analyses

For mice in various groups, the statistical values were represented as means  $\pm$  SDs and compared via analysis of variance, and a subsequent post hoc (least significant difference) test. Bielschowsky procedure was employed to semi-quantitate the A $\beta$  plaques.<sup>32</sup> The correlation of the level of  $\alpha 7$  nAChR protein with spatial learning and memory was analysed employing the Pearson correlation test. SPSS 22.0 (SPSS Inc.) was used to carry out all analyses, and  $p$  values of  $<0.05$  were regarded significantly different.

## 3 | RESULTS

### 3.1 | Confirmation of the APP/PS1 murine genotype

As shown in Figure S1, when the PCR amplification template was genomic DNA, the transgenic group exhibited products (sizes around 400 and 600 bp) that coincided separately with the APP and PS1 genes in size. However, this was not observed among the WT mice.

### 3.2 | Spatial learning and memory in mice

According to the Morris water maze results displayed in Figure 1, both the number of times the original facility location was crossed and the

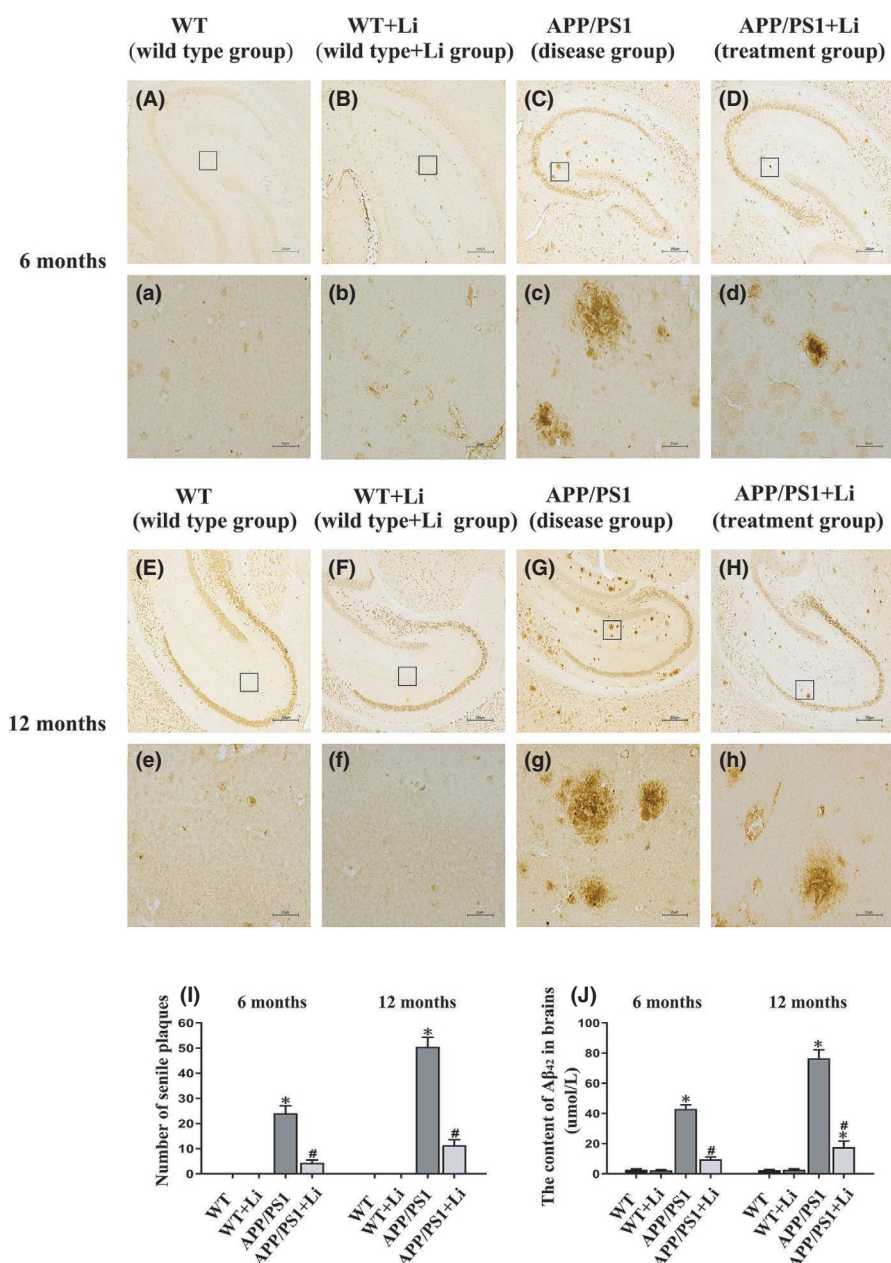


**FIGURE 2** Senile plaques in the cerebral zone of 6- (A–D, a–d) and 12-month-old (E–H, e–h) WT and dual-transgenic APP/PS1 mice. The four groups were subjected to 2-month gavage administration once daily as follows: WT: WT mice received physiological saline (PS); WT+Li: WT mice received LiCl (Li); APP/PS1: APP/PS1 mice received PS; APP/PS1+Li: APP/PS1 mice received Li. A, a, E and e: the WT group; B, b, F and f: the WT+Li group; C, c, G and g: the APP/PS1 group; D, d, H and h: the APP/PS1+Li group. The quantitative data presented were obtained from six mice each group. Under light microscope with  $40\times$ , five non-overlapping visual fields were randomly selected and counted from each section. Magnification: A–H,  $40\times$ , scale bar =  $250\ \mu\text{m}$ ; a–h (magnification of the squares in A–H),  $400\times$ , scale bar =  $25\ \mu\text{m}$ . I: the number of senile plaques identified via immunohistochemistry. J: The content of A $\beta_{42}$  in the brain as assayed by ELISA. The values are represented as means  $\pm$  SDs ( $n = 6$ ),  $*p < 0.05$  as compared to WT;  $\#p < 0.05$  as compared to APP/PS1 mice

time expenditure at this location were reduced, while the escape latency was increased in the 6- and 12-month-old APP/PS1 mice as compared to the corresponding WT mice. Treatment for the transgenic animals with LiCl for 2 months beginning at 4 or 10 months of age clearly improved both their learning capability and memory function.

### 3.3 | Senile plaque count and level of Aβ<sub>42</sub> in the cortex of mouse brains

The brains of 6- (Figure 2A–D and a–d) or 12-month-old (Figure 2E–H and e–h) transgenic mice contained Aβ-immunoreactive senile plaques, the number of which was markedly reduced by exposure to LiCl beginning at either 6 or 12 months of age. There were no detectable amyloid plaques in the cerebral zone of WT mice with or without exposure LiCl (Figure 2I).

The cortex of WT mice contained a very low level of Aβ<sub>42</sub> that was unaffected by treatment with LiCl. In contrast, this level was much higher in untreated APP/PS1 animals, where the level was decreased even further by treatment with LiCl (Figure 2J).

### 3.4 | Primary neuronal viability upon AβOs, LiCl and/or XAV939 exposures

As shown in Figure S2A–E, the immunostaining analysis of the primary neurons cultured using antibody, which were prepared from the cerebral hippocampal zone of neonatal rats, directed towards DAPI (a nucleus marker), GFAP (an astrocyte marker) and NeuN (a neuron marker), suggesting that these cells (about 90%) were neuronal. These primary neurons were assessed for viability following

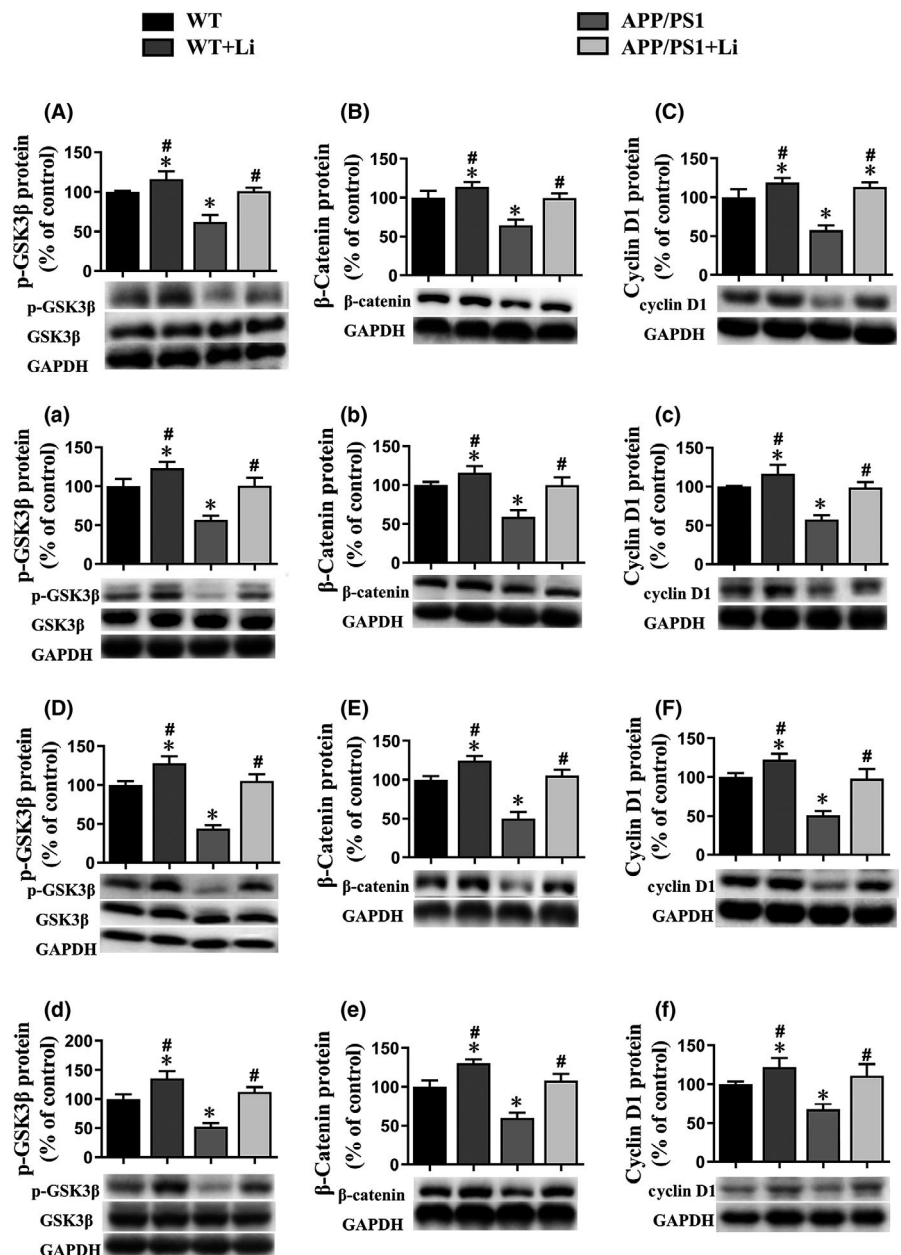


**FIGURE 3** Expression of the p-GSK3β, β-catenin and cyclin D1 proteins in the hippocampus (A–F) and cortex (a–f) of the brains of 6- (A–C and a–c) or 12-month-old (D–F and d–f) WT and dual-transgenic APP/PS1 mice. The four groups were subjected to 2-month gavage administration once daily as follows: WT: WT mice received physiological saline (PS); WT+Li: WT mice received LiCl (Li); APP/PS1: APP/PS1 mice received PS; APP/PS1+Li: APP/PS1 mice received Li. The values are represented as means ± SDs (n = 6), \*p < 0.05 as compared to WT; #p < 0.05 as compared to APP/PS1 mice

exposure to A $\beta$ Os, LiCl and/or XAV939 utilizing the CCK-8 test. Treatment with 10 mmol/L LiCl for 6 h or 1  $\mu$ mol/L XAV939 for 24 h did not cause any significant cytotoxicity (Figure S2F,G). Exposure of these primary neurons to 0.5  $\mu$ mol/L A $\beta$ Os for 48 h (conditions chosen on the basis of an earlier study;<sup>33</sup>) reduced cell viability, a reduction that was attenuated by LiCl, but aggravated by XAV939 (Figure S2H).

### 3.5 | Expression of proteins involved in Wnt signalling in the hippocampus and cortex of mouse brains and primary neurons

As Western blotting revealed, the phosphor-GSK3 $\beta$  (ser9) (not total GSK3 $\beta$ ),  $\beta$ -catenin and cyclin D1 levels in the cerebral hippocampus (Figure 3A–C and D–F) or cortex (Figure 3a–c and d–f) of the APP/PS1 mice aged 6 (Figure 3A–C and a–c) or 12 (Figure 3D–F and d–f) months were all lower than the corresponding levels in the WT mice.

Noteworthy is that such declines were mitigated by LiCl treatment for transgenic mice.

With regard to primary neurons, the levels of the  $\beta$ -catenin and cyclin D1 proteins were enhanced by exposure to LiCl alone, whereas XAV939 reduced these levels. Exposure of primary neurons to A $\beta$ Os alone also reduced these levels, an effect that was attenuated by LiCl and enhanced by XAV939 (Figure 4A,B).

Compared to the corresponding controls, transfection of primary neurons with siRNA targeting the  $\beta$ -catenin gene reduced both the level of this protein and that of cyclin D1 (Figure 4E,F).

### 3.6 | Expression of $\alpha$ 7 nAChR mRNA and protein in the hippocampus and cortex of mouse brains and primary neurons

In comparison with the corresponding control group, the levels of both  $\alpha$ 7 nAChR protein and mRNA were enhanced by

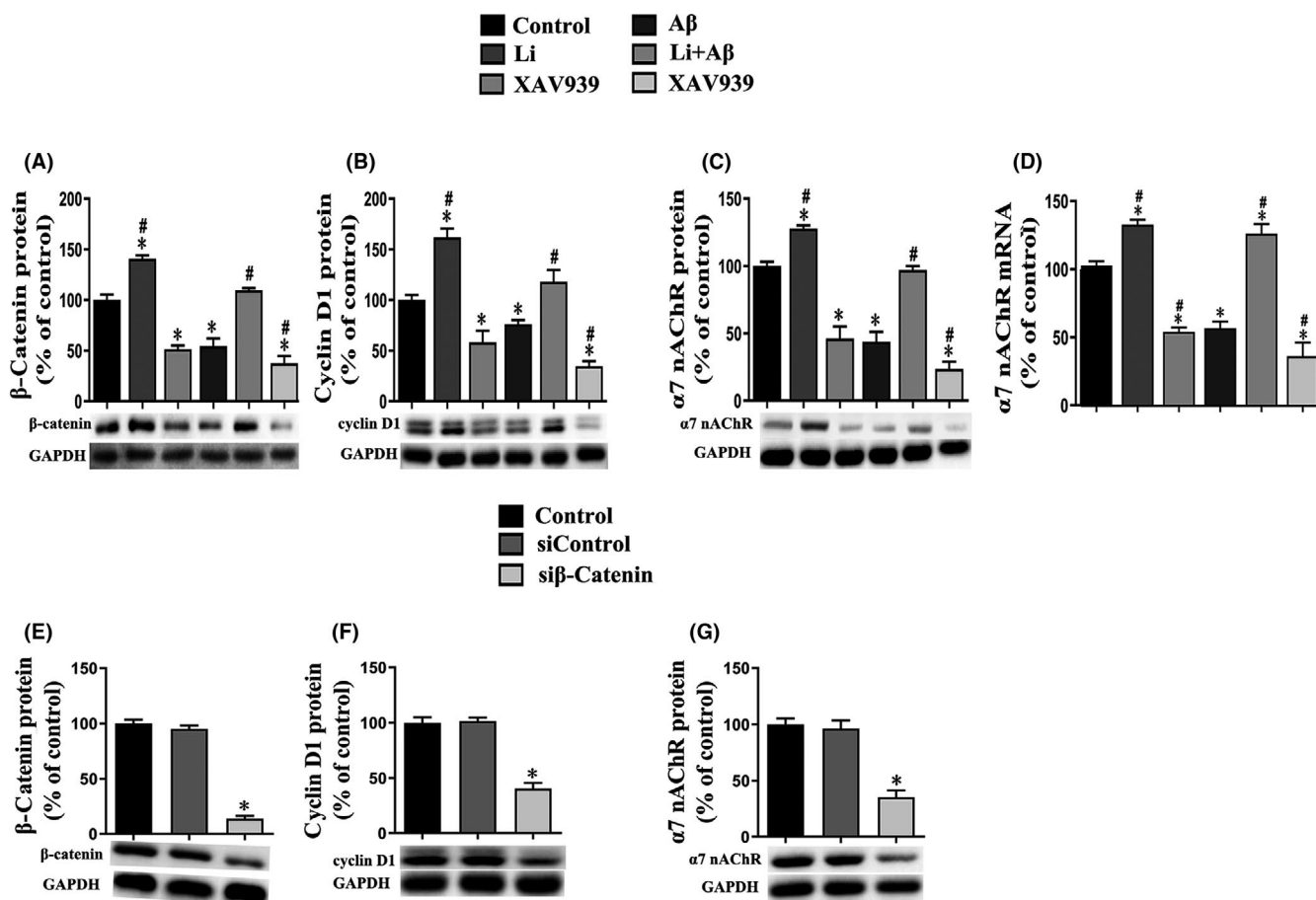


**FIGURE 4** Expression of the  $\beta$ -catenin (A and E) and cyclin D1 proteins (B and F) and  $\alpha$ 7 nAChR protein and mRNA (C, D and G) by primary hippocampus neurons. control: untreated primary neurons; Li: primary neurons exposed to LiCl (10 mmol/L) for 6 h; XAV939: primary neurons exposed to XAV939 (1  $\mu$ mol/L) for 24 h; A $\beta$ : primary neurons exposed to A $\beta$ Os (0.5  $\mu$ mol) for 48 h; Li+A $\beta$ : primary neurons exposed to LiCl and A $\beta$ Os; XAV939+A $\beta$ : primary neurons exposed to XAV939 and A $\beta$ Os; sicontrol: primary neurons transfected with sicontrol; si $\beta$ -catenin: primary neurons transfected with small interfering RNA (siRNA) targeting the  $\beta$ -catenin gene for 48 h. The values presented are the means  $\pm$  SDs from three separate experiments. \* $p$  < 0.05 as compared to control group; # $p$  < 0.05 as compared to the A $\beta$  group

exposure of the neurons to LiCl alone and reduced by XAV939. Moreover, these levels were reduced by exposure to A $\beta$ O<sub>s</sub>, a decline that was attenuated by LiCl, but enhanced by XAV939 (Figure 4C,D).

Moreover, transfection of neurons with siRNA targeting the  $\beta$ -catenin gene reduced the level of this protein, as well as that of  $\alpha$ 7 nAChR (Figure 4G).

According to the results of real-time PCR and Western blotting, declines in the protein (Figure 5A–D) and mRNA (Figure 5E–H) levels of  $\alpha$ 7 nAChR were noted in the hippocampus (Figure 5A,C,E,G) and cortex (Figure 5B,D,F,H) of APP/PS1 mice at 6 (Figure 5A,B,E,F) and 12 (Figure 5C,D,G,H) months of age. Administration of LiCl to either the WT or APP/PS1 animals elevated these levels in both of these areas of the brain.

Semiquantitative immunohistochemical analysis of mouse brains revealed localization of  $\alpha$ 7 nAChR primarily at the plasma membrane and axon (Figure 6A–D and a–d). This immunostaining was less intense in the hippocampus (Figure 6A,a,C,c) and cortex (Figure 6B,b,D,d) of the APP/PS1 mice at 6 (Figure 6A,a,B,b) and 12 (Figure 6C,c,D,d) months of age than for the WT group. In both groups of animals, LiCl augmented the intensity of this staining.

In the case of primary neurons, semiquantitative immunofluorescent analysis revealed localization of the  $\alpha$ 7 nAChR subunit mainly at the plasma membrane and axon (Figure 7A). Exposure to LiCl alone enhanced this immunofluorescence, whereas XAV939 reduced it. Interestingly, the reduction caused by A $\beta$ O<sub>s</sub> alone was attenuated by LiCl and enhanced by XAV939 (Figure 7D).

### 3.7 | Correlations between the $\alpha$ 7 nAChR level and spatial learning and memory

Correlation analysis revealed a negative association between the elevated level of  $\alpha$ 7 nAChR protein present in the cerebral zone of APP/PS1 mice aged 6 (Figure S3A,C) or 12 (Figure S3B,D) months following exposure to LiCl and the impairment in their spatial learning and memory.

## 4 | DISCUSSION

In the cerebral zone of APP/PS1 mice, one most common animal AD model, the content of A $\beta$  and number of senile plaques are elevated, while the learning capability and memory function of these mice are impaired.<sup>34</sup> Here, we found that in the cerebral zone of 6- and, especially, 12-month-old mice of this strain, the increases in size and quantity of senile plaques were evident and learning and memory significantly impaired. Consistent with previous studies,<sup>25,26</sup> we have also confirmed that A $\beta$  damages neurons directly, both in vitro and in vivo, leading to dysfunction and apoptosis.

$\alpha$ 7 nAChR is widespread throughout the central nervous system. Regarding the well-defined intracerebral functions of  $\alpha$ 7 nAChR, it can modulate synaptic plasticity and transmission that underlay ordinary processes of cognition, attention, learning and memory.<sup>35,36</sup> In our current investigation, the protein expression of  $\alpha$ 7 nAChR in the cerebral hippocampus and cortex of APP/PS1 mice aged 6 and 12 months was found to be lower than in WT animals. In addition,

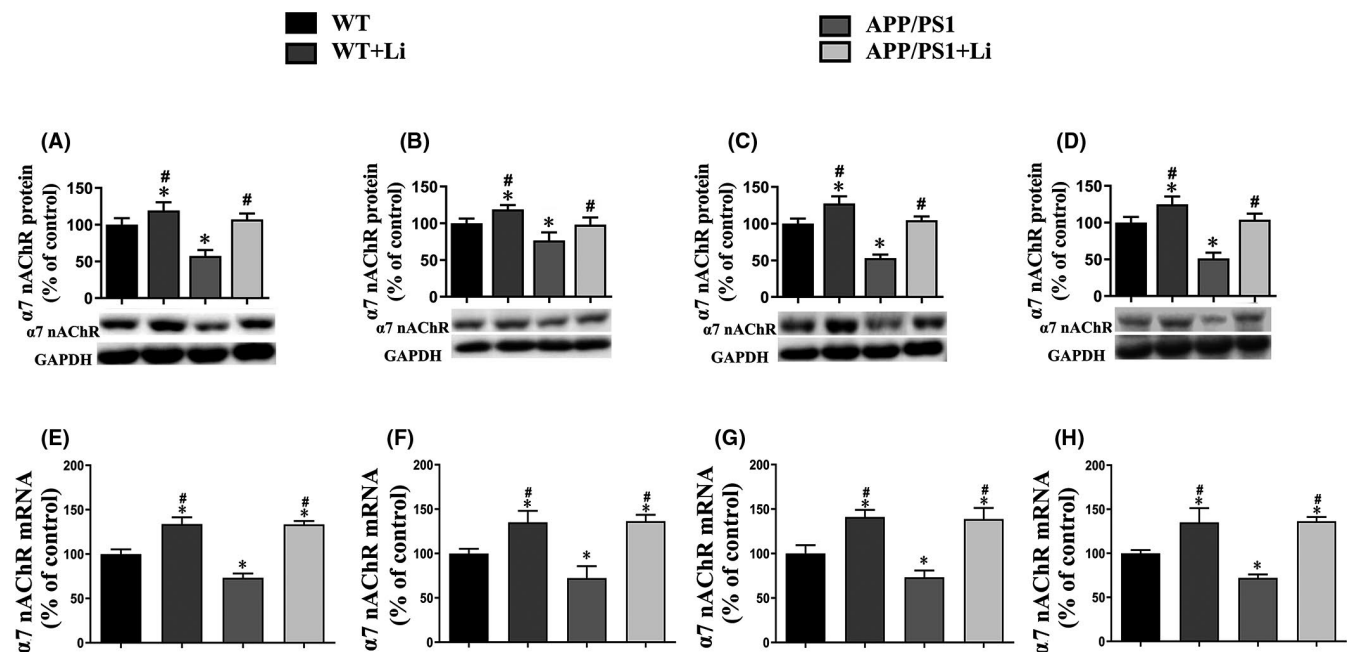


**FIGURE 5** Protein and mRNA expressions of  $\alpha$ 7 nAChR in the hippocampus (A, C, E and G) and cortex (B, D, F and H) of the brains of 6- (A, B, E and F) and 12-month-old (C, D, G and H) WT and dual-transgenic APP/PS1 mice. The four groups were subjected to 2-month gavage administration once daily as follows: WT: WT mice received physiological saline (PS); WT+Li: WT mice received LiCl (Li); APP/PS1: APP/PS1 mice received PS; APP/PS1+Li: APP/PS1 mice received Li. The values are represented as means  $\pm$  SDs ( $n = 6$ ), \* $p < 0.05$  as compared to WT; # $p < 0.05$  as compared to APP/PS1 mice

primary neurons exposed to A $\beta$ O show a tendency towards reduced expression of  $\alpha$ 7 nAChR. Furthermore, we confirmed the damaging effect of A $\beta$  on  $\alpha$ 7 nAChR both in vivo and in vitro, as well as the relationship between the loss of  $\alpha$ 7 nAChR and the decline in the learning capability and memory function for APP/PS1 mice. Computational modelling indicates that arginine-208 and glutamate-211 in  $\alpha$ 7

nAChR are involved in their interaction with A $\beta$ .<sup>37</sup> Moreover, our previous results showed that the loss of the ability of learning and memory of APP/PS1 mice can be reversed or aggravated via activation or suppression of  $\alpha$ 7 nAChR expression, respectively.<sup>38</sup>

At the same time, we found that the loss of  $\alpha$ 7 nAChR is associated with a reduction in the level of the  $\beta$ -catenin protein. The

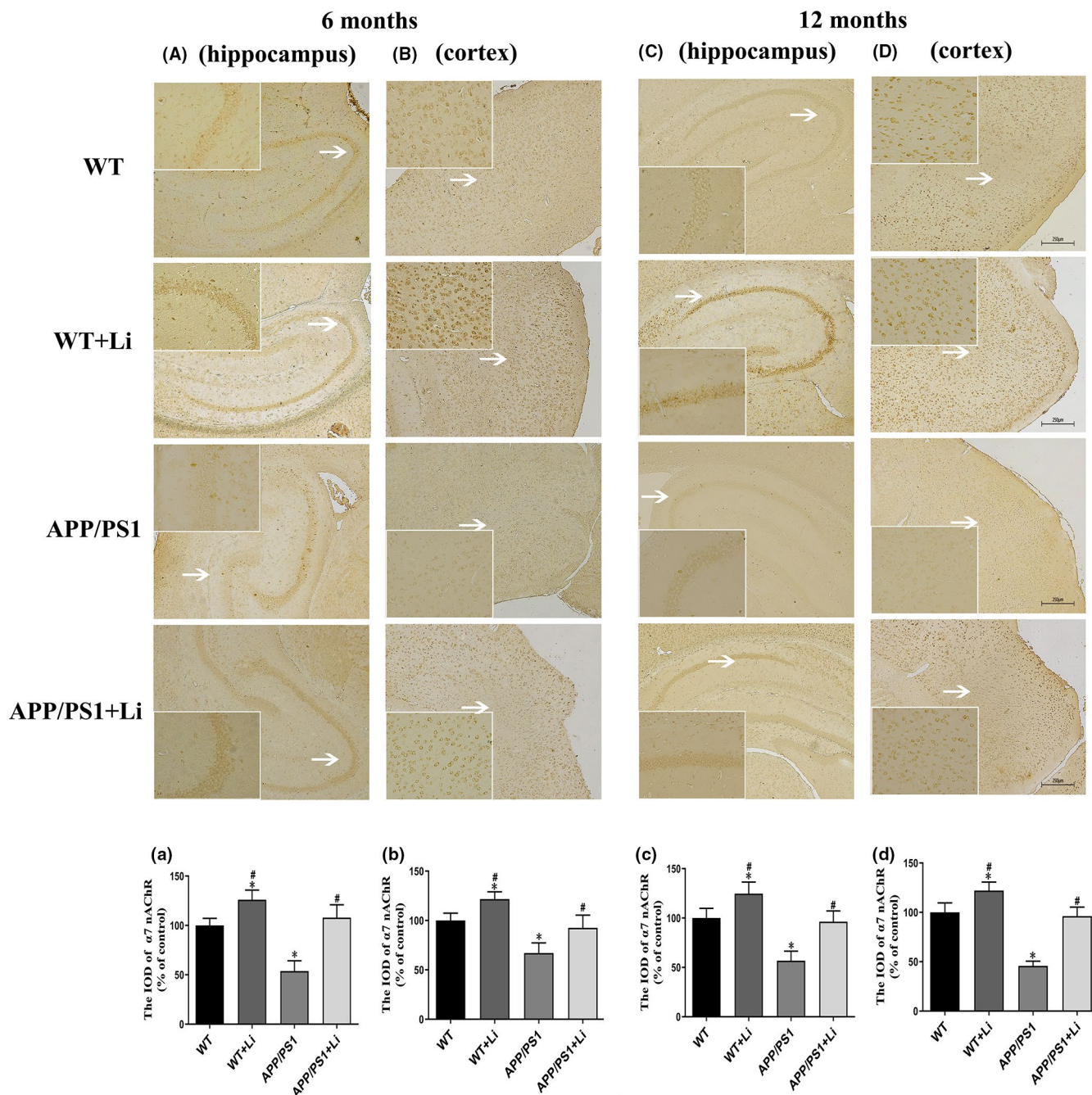


**FIGURE 6** Immunohistochemical staining for  $\alpha$ 7 nAChR protein in the hippocampus (A and C) and cortex (B and D) of the brains of 6- (A and B) and 12-month-old (C and D) WT and dual-transgenic APP/PS1 mice. The four groups were subjected to 2-month gavage administration once daily as follows: WT: WT mice received physiological saline (PS); WT+Li: WT mice received LiCl (Li); APP/PS1: APP/PS1 mice received PS; APP/PS1+Li: APP/PS1 mice received Li. Magnification: A–D, 40 $\times$ , scale bar = 250  $\mu$ m or 200 $\times$  (magnification of the white arrows in A–D). a–d: semiquantitative analysis of the integrated optical density (IOD) of  $\alpha$ 7 nAChR staining in the hippocampus (a, c) and cortex (b, d) of the 6- (a, b) and 12-month-old (c, d) mice in the different groups. The values are represented as means  $\pm$  SDs ( $n = 6$ ), \* $p < 0.05$  as compared to WT; # $p < 0.05$  as compared to APP/PS1 mice

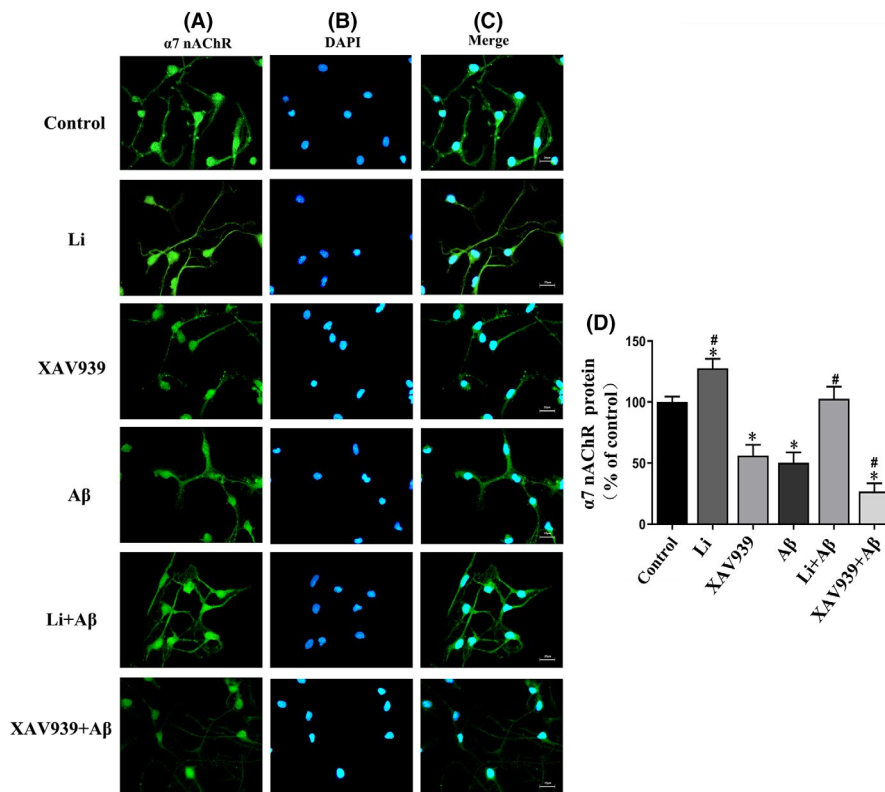


**FIGURE 7** Immunofluorescent staining for  $\alpha 7$  nAChR protein in primary hippocampus neurons. Control group: untreated primary neurons; Li: primary neurons exposed to LiCl (10 mmol/L) for 6 h; XAV939: primary neurons exposed to XAV939 (1  $\mu$ mol/L) for 24 h; A $\beta$ : primary neurons exposed to A $\beta$ O (0.5  $\mu$ mol) for 48 h; Li+A $\beta$  group: primary neurons exposed to LiCl and A $\beta$ O; XAV939+A $\beta$  group: primary neurons exposed to XAV939 and A $\beta$ O. The neurons were stained using rabbit antibody against  $\alpha 7$  nAChR (green), while staining of cellular nuclei was accomplished using DAPI (blue). D: semiquantitative analysis of the integrated optical density (IOD) for  $\alpha 7$  nAChR staining. Magnification: 400 $\times$ , scale bar = 25  $\mu$ m. The values are represented as the means  $\pm$  SDs from three separate experiments. \* $p$  < 0.05 as compared to the control group; # $p$  < 0.05 as compared to the A $\beta$  group

decline of learning and memory in patients with AD also appears to be associated with the decrease of Wnt/ $\beta$ -catenin in their brain.<sup>39</sup> In animal models as well, the AD pathology is strongly correlated with the down-regulation of Wnt/ $\beta$ -catenin axis.<sup>12</sup> Accordingly, the Wnt/ $\beta$ -catenin signal pathway offers a therapeutic target for alleviating the pathological process that results in AD.<sup>40</sup> In the present case, we verified that Wnt/ $\beta$ -catenin signalling in the APP/PS1 murine cerebral zone or in the primary neurons exposed to A $\beta$ O *in vitro* is evidently weaker than in the WT mice or unexposed cells.

Evidence for a neuroprotective effect of lithium has accumulated over the last two decades,<sup>41</sup> and this element has been found to be involved in the regulation of numerous genes, proteins and metabolites.<sup>42</sup> Most noteworthy of these is the inhibition of GSK3 $\beta$  by lithium, which has a wide range of beneficial effects.<sup>43</sup> Consistent with previous findings,<sup>44</sup> we found here that LiCl enhances the learning capability and memory function of APP/PS1 mice aged both 6 and 12 months.

Moreover, both the elevated content of A $\beta$ <sub>42</sub> and the size or quantity of senile plaques in the cerebral zone of these transgenic mice were reduced through treatment with LiCl. In addition, this reduction in A $\beta$  content was correlated to an improvement in learning and memory. Some evidence from animal models of AD indicates that LiCl

can prevent neurotoxicity by reducing the production of A $\beta$ ,<sup>45</sup> as well as that the cognitive benefits of LiCl are associated with enhanced clearance of A $\beta$  via up-regulation of brain microvascularization by lipoprotein receptor-related protein 1 and increased bulk flow of cerebrospinal fluid.<sup>46</sup> In human neuronal cells, LiCl alters proteins such as the rab proteins, which have been implicated in the processing of APP in connection with the pathophysiology of AD.<sup>47</sup> In addition, up-regulation of Wnt/ $\beta$ -catenin signalling by LiCl can cause  $\beta$ -catenin to bind specifically to regions within the BACE1 promoter that contain putative TCF/LEF motifs and repress transcription.<sup>33</sup> Any of these mechanisms may explain the reduction in A $\beta$  caused by lithium.

LiCl is a classic agonist of the Wnt/ $\beta$ -catenin pathway, which is the main reason it has been chosen for testing as a candidate drug for treating AD in numerous studies.<sup>10,22</sup> Here, up-regulation of the Wnt/ $\beta$ -catenin axis by LiCl in 6- and 12-month-old mice with or without the APP/PS1 double mutation was verified. This effect was associated with inactivation of GSK3 $\beta$  through specific phosphorylation of Ser9 in its N-terminus,<sup>48</sup> which elevates the levels of the  $\beta$ -catenin and cyclin D1 proteins. In addition, we found here that in primary hippocampal neurons the Wnt/ $\beta$ -catenin pathway was activated by LiCl and inactivated by XAV939 or A $\beta$ O. Importantly, this effect by A $\beta$ O could be attenuated by LiCl, but aggravated by XAV939.

In line with these findings *in vitro*, the Wnt/ $\beta$ -catenin axis initiation has been proven to offset the harmful action of  $A\beta O$ ,<sup>40</sup> which thus exerts a probable fundamental effect on maintaining neuronal and synaptic functions.<sup>49</sup> Abundant evidence demonstrates that reactivation of the Wnt/ $\beta$ -catenin pathway completely restores the number of synapses and synaptic plasticity<sup>50</sup> and this pathway is a target for recovery of neuronal circuits following degeneration of synapses.<sup>51</sup> Since  $\alpha 7$  nAChRs are expressed widely on both pre-synaptic and post-synaptic membranes,<sup>14,15</sup> we hypothesize that activation of Wnt/ $\beta$ -catenin pathway by LiCl stabilizes expression of these receptors in the animal AD models' cerebral region.

Interestingly, the reduction in the cerebral  $\alpha 7$  nAChR protein expression could be mitigated by LiCl exposure for the dual-transgenic mice. In addition, in WT animals, treatment with LiCl led to elevated cortical or hippocampal levels of  $\alpha 7$  nAChR protein and mRNA apart from initiating the Wnt/ $\beta$ -catenin axis. These findings indicate that in the course of AD development, LiCl may regulate the  $\alpha 7$  nAChR subunit expression. In this connection, negative association was noted between the increased protein level of  $\alpha 7$  nAChR in the LiCl-treated APP/PS1 murine brains and the impaired spatial learning and memory capabilities of these mice. In combination with previous observations, this study further supports the important role of  $\alpha 7$  nAChR in learning and memory<sup>35,36</sup> and suggests that restoring normal expression of  $\alpha 7$  nAChR may be one mechanism by which LiCl improves learning capability and memory function for APP/PS1 mice.

Subsequently, in primary neurons, it was found that the decrease in the  $\alpha 7$  nAChR subunit expression in these cells induced by  $A\beta O$ s was attenuated by LiCl, but aggravated by XAV939. Furthermore, transfection of primary neurons with siRNA targeting the  $\beta$ -catenin gene lowered not only the level of this protein and its downstream protein cyclin D1, but also reduced the  $\alpha 7$  nAChR subunit levels. The above findings imply that the gene encoding  $\alpha 7$  nAChR is regulated by the Wnt/ $\beta$ -catenin pathway and that the reductions in  $\alpha 7$  nAChR protein and mRNA induced by  $A\beta O$  may be mediated by inactivation of this pathway.

Cholinergic neurons are reliant on ( $\alpha 7$ ) 5 nAChRs for maintaining the ability to learn and memory.<sup>52</sup> At present, relatively little is known about potential interactions between the Wnt/ $\beta$ -catenin pathway and the function of nAChRs. Earlier investigations revealed that the canonical Wnt axis initiation may promote the pre-synaptic localization of  $\alpha 7$ -nAChR<sup>53</sup> and accelerate differentiation of stem cells in adipose tissue into cholinergic neurons.<sup>54</sup> Moreover, activating the canonical Wnt pathway by Wnt-7a has been reported to promote up-regulation and aggregation of  $\alpha 7$  nAChR.<sup>55</sup> These observations are in line with the finding with *C. elegans* that mutations causing defects in the Wnt axis lower the synaptic expression of the ACR-16/ $\alpha 7$  nAChR homolog, a change accompanied by attenuated receptor function and loss of nicotinic-related behaviors.<sup>56</sup>

Interestingly, a possible role for the expression and activity of N-methyl-D-aspartic acid receptors (NMDARs) and glutamatergic transmission was found in the therapeutic effects of lithium.<sup>57</sup> In many cases, the  $\alpha 7$  nAChRs and NMDARs were closely apposed on axon terminals, where  $\alpha 7$  nAChRs may regulate glutamate release

and its subsequent modulation of neuronal plasticity.<sup>58,59</sup> Activating  $\alpha 7$  nAChRs potentiated responses to glutamate by increasing the membrane insertion of NMDARs.<sup>60</sup> However, whether lithium affects  $\alpha 7$  nAChRs signal transduction through NMDARs has not been verified, which is worth of further study.

In the cerebral zone of APP/PS1 mice, the  $A\beta$  level was increased and those of  $\alpha 7$  nAChR, phosphor-GSK3 $\beta$  (ser9),  $\beta$ -catenin and cyclin D1 (protein and/or mRNA levels) were reduced. Treatment with LiCl for 2 months at 4 or 10 months of age attenuated all of these effects. Similar expression variations were observed for these proteins in primary neurons exposed to  $A\beta O$ s, and these effects were attenuated by LiCl and aggravated by XAV939. Inhibition of  $\beta$ -catenin expression lowered the level of  $\alpha 7$  nAChR protein in these cells. A proposed molecular pathway involving above changes is shown in Figure S4. These findings suggest that LiCl can reverse the impairment in learning capability and memory function for APP/PS1 mice via a mechanism that might involve elevation of the level of  $\alpha 7$  nAChR as a result of altered Wnt/ $\beta$ -catenin signalling.

## CONFLICT OF INTEREST

The authors have no conflict of interest to declare.

## AUTHOR CONTRIBUTIONS

Jie Xiang: Formal analysis (equal); Writing-original draft (equal). Longyan Ran: Formal analysis (equal). Xiaoxiao Zeng: Formal analysis (equal). Wenwen He: Formal analysis (equal). Yi Xu: Formal analysis (equal). Kun Cao: Formal analysis (equal). Yangting Dong: Formal analysis (equal). Xiaolan Qi: Formal analysis (equal). Wenfeng Yu: Formal analysis (equal). Yan Xiao: Formal analysis (equal). Zhizhong Guan: Conceptualization (equal); Writing-review & editing (equal).

## DATA AVAILABILITY STATEMENT

All data generated or analysed during this study are included in this published article and its supplementary information files.

## ORCID

Zhi-Zhong Guan  <https://orcid.org/0000-0001-7001-6145>

## REFERENCES

- Schelkens P, De Strooper B, Kivipelto M, et al. Alzheimer's disease. *Lancet*. 2021;397:1577-1590.
- Lashley T, Schott JM, Weston P, et al. Molecular biomarkers of Alzheimer's disease: progress and prospects. *Dis Model Mech*. 2018;11:doi: 10.1242/dmm.031781
- Hampel H, Mesulam M-M, Cuello AC, et al. The cholinergic system in the pathophysiology and treatment of Alzheimer's disease. *Brain*. 2018;141:1917-1933.
- Mitsushima D, Sano A, Takahashi T. A cholinergic trigger drives learning-induced plasticity at hippocampal synapses. *Nat Commun*. 2013;4:2760.
- Lombardo S, Maskos U. Role of the nicotinic acetylcholine receptor in Alzheimer's disease pathology and treatment. *Neuropharmacology*. 2015;96:255-262.
- Guan Z-Z, Zhang X, Ravid R, et al. Decreased protein levels of nicotinic receptor subunits in the hippocampus and temporal cortex of patients with Alzheimer's disease. *J Neurochem*. 2000;74:237-243.

7. Guan ZZ, Miao H, Tian JY, et al. Suppressed expression of nicotinic acetylcholine receptors by nanomolar beta-amyloid peptides in PC12 cells. *J Neural Transm (Vienna)*. 2001;108:1417-1433.
8. Pym L, Kemp M, Raymond-Delpech V, et al. Subtype-specific actions of beta-amyloid peptides on recombinant human neuronal nicotinic acetylcholine receptors (alpha7, alpha4beta2, alpha3beta4) expressed in *Xenopus laevis* oocytes. *Br J Pharmacol*. 2005;146:964-971.
9. Wang HY, Lee DH, D'Andrea MR, et al. beta-Amyloid(1-42) binds to alpha7 nicotinic acetylcholine receptor with high affinity. Implications for Alzheimer's disease pathology. *J Biol Chem*. 2000;275:5626-5632.
10. Clevers H, Nusse R. Wnt/ $\beta$ -catenin signaling and disease. *Cell*. 2012;149:1192-1205.
11. Menet R, Bourassa P, Calon F, et al. Dickkopf-related protein-1 inhibition attenuates amyloid-beta pathology associated to Alzheimer's disease. *Neurochem Int*. 2020;141:104881.
12. Tapia-Rojas C, Inestrosa NC. Loss of canonical Wnt signaling is involved in the pathogenesis of Alzheimer's disease. *Neural Regen Res*. 2018;13:1705-1710.
13. Jia L, Piña-Crespo J, Li Y. Restoring Wnt/ $\beta$ -catenin signaling is a promising therapeutic strategy for Alzheimer's disease. *Mol Brain*. 2019;12:104.
14. Chu ZG, Zhou FM, Hablitz JJ. Nicotinic acetylcholine receptor-mediated synaptic potentials in rat neocortex. *Brain Res*. 2000;887:399-405.
15. Zolles G, Wagner E, Lampert A, et al. Functional expression of nicotinic acetylcholine receptors in rat neocortical layer 5 pyramidal cells. *Cereb Cortex*. 2009;19:1079-1091.
16. Vallée A, Vallée J-N, Guillevin R, et al. Riluzole: a therapeutic strategy in Alzheimer's disease by targeting the WNT/ $\beta$ -catenin pathway. *Aging (Albany NY)*. 2020;12:3095-3113.
17. Jin NA, Zhu H, Liang X, et al. Sodium selenate activated Wnt/ $\beta$ -catenin signaling and repressed amyloid- $\beta$  formation in a triple transgenic mouse model of Alzheimer's disease. *Exp Neurol*. 2017;297:36-49.
18. Nunes PV, Forlenza OV, Gattaz WF. Lithium and risk for Alzheimer's disease in elderly patients with bipolar disorder. *Br J Psychiatry*. 2007;190:359-360.
19. Rybakowski JK. Challenging the negative perception of lithium and optimizing its long-term administration. *Front Mol Neurosci*. 2018;11:349.
20. Wen J, Sawmiller D, Wheeldon B, et al. A review for Lithium: pharmacokinetics, drug design, and toxicity. *CNS Neurol Disord Drug Targets*. 2019;18:769-778.
21. Hampel H, Lista S, Mango D, et al. Lithium as a treatment for Alzheimer's disease: the systems pharmacology perspective. *J Alzheimers Dis*. 2019;69:615-629.
22. Cisternas P, Zolezzi JM, Martinez M, et al. Wnt-induced activation of glucose metabolism mediates the in vivo neuroprotective roles of Wnt signaling in Alzheimer disease. *J Neurochem*. 2019;149:54-72.
23. Shetti D, Zhang B, Fan C, et al. Low dose of paclitaxel combined with XAV939 attenuates metastasis, angiogenesis and growth in breast cancer by suppressing Wnt signaling. *Cells*. 2019;8:892.
24. Zhao L, Gong N, Liu M, et al. Beneficial synergistic effects of microdose lithium with pyrroloquinoline quinone in an Alzheimer's disease mouse model. *Neurobiol Aging*. 2014;35:2736-2745.
25. Xiang J, Cao K, Dong Y-T, et al. Lithium chloride reduced the level of oxidative stress in brains and serums of APP/PS1 double transgenic mice via the regulation of GSK3 $\beta$ /Nrf2/HO-1 pathway. *Int J Neurosci*. 2020;130:564-573.
26. Dong Y-T, Cao K, Tan L-C, et al. Stimulation of SIRT1 attenuates the level of oxidative stress in the brains of APP/PS1 double transgenic mice and in primary neurons exposed to oligomers of the amyloid- $\beta$  peptide. *J Alzheimers Dis*. 2018;63:283-301.
27. Klein WL. Abeta toxicity in Alzheimer's disease: globular oligomers (ADDLs) as new vaccine and drug targets. *Neurochem Int*. 2002;41:345-352.
28. Berardo C, Siciliano V, Di Pasqua LG, et al. Comparison between lipofectamine RNAiMAX and GenMute transfection agents in two cellular models of human hepatoma. *Eur J Histochem*. 2019;63: doi: 10.4081/ejh.2019.3048
29. Cao K, Xiang J, Dong Y-T, et al. Exposure to fluoride aggravates the impairment in learning and memory and neuropathological lesions in mice carrying the APP/PS1 double-transgenic mutation. *Alzheimers Res Ther*. 2019;11:35.
30. Duan JJ, Zhang Q, Hu X, et al. N(4)-acetylcytidine is required for sustained NLRP3 inflammasome activation via HMGB1 pathway in microglia. *Cell Signal*. 2019;58:44-52.
31. Cao K, Dong Y-T, Xiang J, et al. Reduced expression of SIRT1 and SOD-1 and the correlation between these levels in various regions of the brains of patients with Alzheimer's disease. *J Clin Pathol*. 2018;71:1090-1099.
32. Yamamoto T, Hirano A. A comparative study of modified Bielschowsky, Bodian and thioflavin S stains on Alzheimer's neurofibrillary tangles. *Neuropathol Appl Neurobiol*. 1986;12:3-9.
33. Parr C, Mirzaei N, Christian M, et al. Activation of the Wnt/ $\beta$ -catenin pathway represses the transcription of the  $\beta$ -amyloid precursor protein cleaving enzyme (BACE1) via binding of T-cell factor-4 to BACE1 promoter. *FASEB J*. 2015;29:623-635.
34. Shi Q, Chowdhury S, Ma R, et al. Complement C3 deficiency protects against neurodegeneration in aged plaque-rich APP/PS1 mice. *Sci Transl Med*. 2017;9:doi: 10.1126/scitranslmed.aaf6295
35. Kabbani N, Nichols RA. Beyond the channel: metabotropic signaling by nicotinic receptors. *Trends Pharmacol Sci*. 2018;39:354-366.
36. Martín-Sánchez C, Alés E, Balseiro-Gómez S, et al. The human-specific duplicated  $\alpha 7$  gene inhibits the ancestral  $\alpha 7$ , negatively regulating nicotinic acetylcholine receptor-mediated transmitter release. *J Biol Chem*. 2021;296:100341.
37. Roberts JP, Stokoe SA, Sathler MF, et al. Selective coactivation of  $\alpha 7$ - and  $\alpha 4\beta 2$ -nicotinic acetylcholine receptors reverses beta-amyloid-induced synaptic dysfunction. *J Biol Chem*. 2021;296:100402.
38. Cao K, Dong Y-T, Xiang J, et al. The neuroprotective effects of SIRT1 in mice carrying the APP/PS1 double-transgenic mutation and in SH-SY5Y cells over-expressing human APP670/671 may involve elevated levels of  $\alpha 7$  nicotinic acetylcholine receptors. *Aging (Albany NY)*. 2020;12:1792-1807.
39. Folke J, Pakkenberg B, Brudek T. Impaired Wnt signaling in the prefrontal cortex of Alzheimer's disease. *Mol Neurobiol*. 2019;56:873-891.
40. Huang M, Liang Y, Chen H, et al. The role of fluoxetine in activating Wnt/ $\beta$ -catenin signaling and repressing  $\beta$ -amyloid production in an Alzheimer mouse model. *Front Aging Neurosci*. 2018;10:164.
41. Rybakowski JK, Suwalska A, Hajek T. Clinical perspectives of Lithium's neuroprotective effect. *Pharmacopsychiatry*. 2018;51:194-199.
42. Roux M, Dosseto A. From direct to indirect lithium targets: a comprehensive review of omics data. *Metalomics*. 2017;9:1326-1351.
43. Sofola-Adesakin O, Castillo-Quan JI, Rallis C, et al. Lithium suppresses A $\beta$  pathology by inhibiting translation in an adult *Drosophila* model of Alzheimer's disease. *Front Aging Neurosci*. 2014;6:190.
44. Rivera DS, Lindsay C, Codocedo JF, et al. Andrographolide recovers cognitive impairment in a natural model of Alzheimer's disease (*Octodon degus*). *Neurobiol Aging*. 2016;46:204-220.
45. Phiel CJ, Wilson CA, Lee VM, et al. GSK-3 $\alpha$  regulates production of Alzheimer's disease amyloid-beta peptides. *Nature*. 2003;423:435-439.
46. Pan Y, Short JL, Newman SA, et al. Cognitive benefits of lithium chloride in APP/PS1 mice are associated with enhanced brain clearance of  $\beta$ -amyloid. *Brain Behav Immun*. 2018;70:36-47.
47. Thompson AJ, Williamson R, Schofield E, et al. Quantitation of glycogen synthase kinase-3 sensitive proteins in neuronal membrane rafts. *Proteomics*. 2009;9:3022-3035.
48. Sutherland C, Leighton IA, Cohen P. Inactivation of glycogen synthase kinase-3 beta by phosphorylation: new kinase connections

- in insulin and growth-factor signalling. *Biochem J.* 1993;296(Pt 1):15-19.
49. Arrázola MS, Silva-Alvarez C, Inestrosa NC. How the Wnt signaling pathway protects from neurodegeneration: the mitochondrial scenario. *Front Cell Neurosci.* 2015;9:166.
  50. Marzo A, Galli S, Lopes D, et al. Reversal of synapse degeneration by restoring Wnt signaling in the adult hippocampus. *Curr Biol.* 2016;26:2551-2561.
  51. Cisternas P, Oliva CA, Torres VI, et al. Presymptomatic treatment with andrographolide improves brain metabolic markers and cognitive behavior in a model of early-onset Alzheimer's disease. *Front Cell Neurosci.* 2019;13:295.
  52. Dineley KT. Beta-amyloid peptide–nicotinic acetylcholine receptor interaction: the two faces of health and disease. *Front Biosci.* 2007;12:5030-5038.
  53. Fariás GG, Vallés AS, Colombres M, et al. Wnt-7a induces presynaptic colocalization of alpha 7-nicotinic acetylcholine receptors and adenomatous polyposis coli in hippocampal neurons. *J Neurosci.* 2007;27:5313-5325.
  54. Liu B, Deng C, Zhang Y, et al. Wnt3a expression during the differentiation of adipose-derived stem cells into cholinergic neurons. *Neural Regen Res.* 2012;7:1463-1468.
  55. Inestrosa NC, Godoy JA, Vargas JY, et al. Nicotine prevents synaptic impairment induced by amyloid- $\beta$  oligomers through  $\alpha$ 7-nicotinic acetylcholine receptor activation. *Neuromolecular Med.* 2013;15:549-569.
  56. Jensen M, Hoerndli FJ, Brockie P, et al. Wnt signaling regulates acetylcholine receptor translocation and synaptic plasticity in the adult nervous system. *Cell.* 2012;149:173-187.
  57. Ghasemi M, Dehpour AR. The NMDA receptor/nitric oxide pathway: a target for the therapeutic and toxic effects of lithium. *Trends Pharmacol Sci.* 2011;32:420-434.
  58. Zappettini S, Grilli M, Olivero G, et al. Nicotinic  $\alpha$ 7 receptor activation selectively potentiates the function of NMDA receptors in glutamatergic terminals of the nucleus accumbens. *Front Cell Neurosci.* 2014;8:332.
  59. Salamone A, Zappettini S, Grilli M, et al. Prolonged nicotine exposure down-regulates presynaptic NMDA receptors in dopaminergic terminals of the rat nucleus accumbens. *Neuropharmacology.* 2014;79:488-497.
  60. Grilli M, Summa M, Salamone A, et al. In vitro exposure to nicotine induces endocytosis of presynaptic AMPA receptors modulating dopamine release in rat nucleus accumbens nerve terminals. *Neuropharmacology.* 2012;63:916-926.

## SUPPORTING INFORMATION

Additional supporting information may be found in the online version of the article at the publisher's website.

**How to cite this article:** Xiang J, Ran L-Y, Zeng X-X, et al. LiCl attenuates impaired learning and memory of APP/PS1 mice, which in mechanism involves  $\alpha$ 7 nAChRs and Wnt/ $\beta$ -catenin pathway. *J Cell Mol Med.* 2021;25:10698–10710. doi:[10.1111/jcmm.17006](https://doi.org/10.1111/jcmm.17006)